EARTHQUAKE RESISTANT DESIGN OF COHESIVE EARTH SLOPES

G. R. Martin* and P. W. Taylor*

Introduction

As many major slope failures have occurred during medium and strong earthquakes, the assessment of the seismic stability of slopes in earthquake-prone areas is of great concern to engineers. Prior to 1964, little attention was given to the development of rational aseismic design methods for earth slopes. Most design methods were based on a static analysis used in conjunction with an arbitrarily selected lateral force acting on the slope with soil strengths determined by conventional laboratory tests. However, the catastrophic slope failures which occurred during the Alaskan earthquake of 1964, resulted in a considerable reappraisal of such static design methods. In recent years significant progress has been made in developing new methods of laboratory testing to determine dynamic soil properties, improved techniques of analysing the dynamic response of slopes and embankments to earthquakes, and new concepts of aseismic design methods for earth slopes. Although research has yet to provide all the answers, the current state of knowledge at least provides an improved guide to engineering judgement in the assessment of the stability of earth slopes during earthquakes.

The problems of slope instability during earthquakes may be placed into three broad categories:

1. Shallow surface slides in slopes of dry cohesionless soils.

2. Slides caused by liquefaction of saturated cohesionless soils, which may be subdivided into :-

   (a) Flow slides caused by liquefaction of large deposits of cohesionless soils.
   (b) Slides caused by liquefaction of thin seams or lenses of sand.

3. Slides in cohesive soils.

Seed (1967) has presented a comprehensive state of the art review where the nature of such slides are described, and problems associated with earthquake stability analyses presented. The majority of catastrophic slides occurring in past earthquakes, such as the extensive slides which occurred during the Alaskan earthquake, fall into the second category noted above. Relatively few slides in cohesive earth slopes resulting from an earthquake are reported in the literature. One of the few slides reported is the bank failure of a section of the All America Canal, which occurred during the 1940 El Centro Earthquake. The extent of the movement is shown in Fig. 1. There have, however, been many reports of subsidence of road and rail embankments founded on soft cohesive soils. e.g. Inangahua, 1968 (Douglas, 1968), Alaska, 1964 (Seed, 1970). The lack of case histories is probably due to the fact that only with low static factors of safety will significant slides be induced in cohesive slopes, and that slumping movements characteristic of such slides might generally not be considered important in comparison with other earthquake damage. However, it is apparent that when such slides occur in motorway cuttings, railway embankments, or earth dams, they result in serious disruption of essential transportation routes, and possible loss of life in the case of earth dams.

In this paper, the problem of the earthquake resistant design of cohesive earth slopes is considered in detail, with particular reference to slopes in saturated clays.

Response of Embankments and Earth Slopes to Earthquakes

Although earth structures are often assumed to act as rigid bodies for the purpose of aseismic design, their behaviour during earthquakes is in fact governed by their dynamic response characteristics. As such characteristics determine the magnitude and distribution of accelerations and stresses acting within the earth structure during an earthquake, dynamic analyses are an important part of the overall assessment of seismic stability. The dynamic earthquake response is controlled by the nature of soils within and beneath the slope or embankment (that is their deformation characteristics under cyclic loading) the height and geometric characteristics of the slope or embankment, and the depth of foundation soils.

Cohesive earth slopes and embankments are often non homogeneous and deform as inelastic and non-linear materials. As a result, dynamic response analyses necessitate many simplifying assumptions. In particular, most published solutions assume a two-dimensional structure (that is, infinitely long) with materials assumed linearly elastic, and energy dissipation resulting from equivalent viscous damping. Dynamic earthquake response analyses for earth dams or embankments have been improved progressively since first appearing in the literature in 1936, recent developments being discussed by Martin (1967), Chopra (1967), Ambraseys and Sarma (1967) and Chopra et. al. (1969). Solutions for the dynamic earthquake response of earth slopes however, have only recently been considered, for it has only been in recent years, with the development of finite element

* Senior Lecturer, Department of Civil Engineering, University of Auckland.

methods of analysis, that solutions have become possible.

In the finite element approach, the earth structure is replaced by a network of triangular linear elastic elements interconnected at a finite number of modal points as shown in Fig. 2. By assuming a particular strain distribution within each element (say constant or linear), element stiffness characteristics may be determined and a stiffness matrix computed for the complete element assemblage. Also, by lumping the mass of each element at the nodal points, a mass matrix can be formulated, and hence natural frequencies and mode shapes for the section can be computed using the standard methods for multi-degree-of-freedom systems. Having established the natural frequencies and mode shapes, the earthquake response for both vertical and horizontal ground accelerations can be obtained by standard modal superposition techniques. Analyses yield complete time histories of displacement, velocity, acceleration, stresses and strains at the nodal points (for the assumed equivalent viscous damping factors). Also time histories of net inertia force acting on any potential sliding mass may be determined. The use of the method for earth slopes has been described by Idriss and Seed (1967), Idriss (1968), and Idriss, Seed and Dezfulian (1969).

To illustrate the effects of dynamic earth slope response to an earthquake ground motion, an example is taken from the paper by Idriss and Seed (1967). The earthquake ground motion shown in Fig. 3 was applied as a base motion to the 50 ft. high earth bank shown in Fig. 2 and the dynamic response computed using the finite element method with an element network as shown in the figure. Material properties used were:

Youngs modulus $E = 2 \times 10^6$ p.s.f.
(Typical of stiff cohesive soils)
Poisson's ratio $\mu = 0.45$ and unit weight $\gamma =$ 120 lb/cu.ft.

An equivalent viscous damping factor of 0.20 was used in each mode. The fundamental period of the bank was computed to be 0.89 seconds. The dynamic stresses resulting from the earthquake at three typical points in the earth bank are shown in Fig. 4, while Fig. 5 shows the variation of maximum surface accelerations. It should be noted that the magnification of horizontal base accelerations at points remote from the slope equals that which would be obtained for the response of a horizontal soil layer using the shear deformation theory described by Idriss and Seed (1968). The calculated fundamental periods of horizontal layers 50 ft. and 100 ft thick comprising the same material are 0.46 seconds and 0.92 seconds respectively. The high magnification of motion over the 50 ft layer is due to the fact that its fundamental period corresponds closely to the period giving the peak acceleration in the El Centro acceleration response spectrum. It has been shown that the response to the vertical ground motion has little effect on the magnitude of the horizontal motions in the slope.

As it is desirable to duplicate earthquake loading conditions on laboratory soil samples in order to assess strength and deformation characteristics under dynamic stress, it is of interest to examine changes in both the magnitude and direction of principal stresses during the earthquake. Consider for example, point F shown in Fig. 4, which is assumed to be on a critical failure surface. The horizontal earthquake acceleration has maximum values (in each direction) at 2.0 and 2.2 seconds after the onset of the earthquake. The average inertia force acting on the sliding mass at these instants is shown in Figure 6(a), expressed as a seismic coefficient. Principal stresses induced by earthquake forces are shown in magnitude and direction in 6(b). These are the superimposed stresses caused by the earthquake. Combining these vectorially with the initial static stresses yields the resultant stresses shown in Figure 6(c). Initial static stresses were obtained from an elastic solution similar to those presented by Duncan and Dunlop (1969). The significance of the stress changes will be discussed later with respect to laboratory testing procedures.

Behaviour of Saturated Cohesive Soils During Dynamic Loading

The majority of dynamic laboratory testing of soils relevant to earthquake problems, has been carried out by means of cyclic load tests in triaxial apparatus. Such apparatus may be stress or strain-controlled, the former being used to examine conditions leading to failure, while the latter is generally used to study deformation behaviour with a view to obtaining equivalent elastic moduli and viscous damping factors for use in earthquake response analyses. Dynamic triaxial apparatus for use in such studies together with typical test results has been described by (among others) Seed (1960), Taylor and Hughes (1965), Seed and Chan (1966), Taylor and Bacchus (1970).

Strength Under Dynamic Loading:

Fig. 7 shows a typical test result from a stress controlled dynamic triaxial test, where a number of cycles of deviator stress* were applied to a sample of an initially anisotropically consolidated saturated clay. Such an initial condition is typical of a soil element in a slope. It is noted that failure (or 20% axial strain) occurred after about 5 cycles, being due to a build up in pore water pressure and associated reduction in strength leading to permanent deformation during the dynamic loading.

Alternatively, samples may be isotropically consolidated, and a static deviator stress applied with the sample undrained, just prior to the dynamic test. If such tests are carried out with a variety of combinations of initial static and dynamic deviator stresses, and the number of cycles to failure noted, the results may be plotted in a non-dimensional form (originated by Seed, 1960) wherein static and dynamic deviator stress, each expressed as a fraction of that causing failure in a static test (i.e. as a fraction of compressive strength) are plotted for various values of N, the number of cycles required to cause failure

* In triaxial tests, the deviator stress is defined as $(\sigma_1 - \sigma_3)$. As changes in all round or hydrostatic pressures do not affect the undrained deformation behaviour of saturated clays, triaxial testing of such materials may be carried out by maintaining σ_3 constant, and applying axial stresses equal to changes in deviator stress occurring in the field.

in the dynamic test.

Figure 8(d) summarizes results of a number of tests saturated compacted samples of a Wanganui clay-silt. For points to the right of the 45° dotted line, the amplitude of cyclic loading is less than the initial static load, and the major principal stress is always vertical. The variation of deviator stress with time for one such test (point 1 in Figure 8(d) is shown in 8(a). The corresponding diagram for point 2, where reversal of deviator stress occurs, is 8(b). Thus, at one part of each cycle, lateral (compressive) stress is greater than that in the axial direction, i.e. the major principal stress, now horizontal, is 90° from its original direction. This results in shear stress reversal on every plane throughout the sample. If stress reversal is not allowed to occur, then a considerably higher maximum deviator stress may be sustained as is shown in 8(c) for point 3. This effect is also apparent, but to a lesser degree, in soils with a higher clay fraction than that used in the test described. (See, for example, Seed and Chan, 1966).

Test results, plotted in the non-dimensional form shown, have been found to be relatively independent of confining pressure and principal stress ratio during consolidation.

Dynamic load-deformation characteristics:

Fig. 9 shows the typical non-linear dynamic load vs. deformation characteristics for a saturated clay, obtained in a strain controlled dynamic test. It is seen that the slope of the loops decreases with time as the pore water pressure increases. From such tests, it is possible to assess equivalent elastic moduli and viscous damping factors for use in elastic response analyses. However, a further difficulty arises in that such parameters vary with strain amplitude. Values of equivalent viscous damping factor may range from 5-20% depending on strain amplitude mobilized during the earthquake response with equivalent elastic moduli decreasing by a factor of 3 or more over the same amplitude range.

The results of such tests as used for elastic response analyses, are discussed by Seed and Idriss (1969) and Parton and Smith (1971).

Laboratory Simulation of Earthquake Loading

In order to simulate earthquake stresses using laboratory triaxial apparatus, several problems arise. As shown in Fig. 6, principal stresses change in both magnitude and orientation during an earthquake, with values varying in an almost random manner throughout the earthquake. Triaxial apparatus provides for either no change in principal stress direction or a 90° change during loading. The latter loading condition is particularly severe, as previously noted. The significance of principal stress re-orientation in the field with reference to the problem of laboratory simulation is now examined.

Consider the stresses at point F, as shown in Fig. 6c. In Fig. 10a, the shear stress τ acting on planes at angle α to the major (static) principal plane is shown for this point. For static conditions, of course, τ has its maximum value when α is 45°. Shear stresses at 2.0 and 2.2 seconds are also shown, with α referred to the same axes. Maximum values are found on planes with α = 28° and 69° respectively. Reversal of shear stress direction occurs only within the zones marked RZ. It should be noted that even at these extreme states, (corresponding to the largest horizontal pulse in each direction, during the entire earthquake record) the maximum static shear stresses do not come within the reversal zones. Also to be noted is that the range of maximum resultant shear stress is not very great.

The problem, then, is to devise a suitable dynamic triaxial test which will have the same effect on sample strength as the variation in stresses within the slope will have on the in situ strength, bearing in mind that, in the triaxial test, principal stress reorientation cannot occur, except through 90°. To ignore principal stress reorientation entirely by considering only the change in maximum resultant shear stress (Fig. 6c), would result in small dynamic stresses being applied and would underestimate the effect of the earthquake. As shown in Fig. 10a, the maximum shear stress varies between 1000 and 1270 lb/sq.ft., a range of only 270 lb/sq.ft. On the other hand, any test in which there is reversal of shear stress on every plane is not representative of field conditions and, as has been shown, is unduly severe.

Strength reduction occurs as a result of an increase in pore water pressure, brought about by the stress changes induced by the earthquake. Hence, as reorientation of principal stress axes is not possible in the test, it is not the resultant stresses which should be applied, but the superimposed stresses (Fig. 6b). The maximum values of superimposed shear stress at 2.0 and 2.2 seconds are, respectively, - 735 and 810 lb/sq. ft., giving a range of 1545 lb/sq.ft. A reasonable simulation of these two maximum earthquake pulses would therefore be to impose, on the sample consolidated under the static principal stresses existing in situ, deviator stress changes which result in these changes in maximum shear stress. It is noted that these values differ very little from the shear stresses acting on the horizontal surface through F, as shown in Fig. 4, viz., - 700 and 800 lb/sq.ft.

In dynamic testing it is convenient to apply a number of symmetrical cycles of dynamic load of equal amplitude, and hence the magnitude and number of cycles which would result in similar deformations to those caused by the almost random series of pulses in the earthquake record must be assessed. Fig. 11 shows the typical logarithmic form of pulse distribution obtained in an earthquake. The graph was developed from the plot of time history of horizontal shear stress at point F shown in Fig. 4. Little research has been carried out on methods of assessing equivalent dynamic loading. However, an applied shear stress amplitude of approximately 2/3 of the maximum amplitude from the earthquake record with the number of cycles being determined by the duration of the earthquake divided by the fundamental period of the structure should provide a conservative approximation. From this the range of maximum shear stress during the test for point F would extend to ± 500 lb/

sq.ft. from the static value, as shown in Fig. 10b.

Concepts of Earthquake Stability Analysis

Pseudo-static Approach:

Many generally accepted methods of assessing the stability of earth slopes and embankments during earthquakes, are based on the use of a static seismic coefficient in conjunction with a conventional slope stability analysis. That is, a minimum factor of safety against sliding is computed for the case where a horizontal static force expressed as the product of a seismic coefficient k and the weight of the potential sliding mass is included in the limiting equilibrium analysis. Generally static strength parameters are used, and the section is usually considered unsafe if the factor of safety approaches unity. In effect, the dynamic forces are replaced by a static force, and hence the approach could be termed a pseudo-static method of analysis.

One of the major problems in the use of this method is the selection of the design seismic coefficient. There appear to be three basic philosophies regarding the meaning of the coefficient selected:

(1) The seismic coefficient could be selected as representing the maximum average acceleration acting on the sliding mass during an earthquake, on the basis that limiting equilibrium should never be exceeded. That is, the development of any permanent deformation, no matter how small, would be considered to constitute a failure.
(2) The seismic coefficient could be chosen to reflect a static acceleration, which would be equivalent in effect to the time-varying lateral accelerations induced during the earthquake; that is, producing the same permanent deformations, and as such, much less than the maximum average acceleration.
(3) The third, and perhaps most common approach is simply to regard the seismic coefficient as an empirical constant which lends to a more conservative design. Empirically chosen values of the order of 0.1 appear to have become traditional through repeated use.

During an earthquake, the lateral forces acting on a slope change in direction and magnitude many times. If the induced dynamic stresses are sufficiently high, permanent deformations of the slope will occur, the overall effect of the cyclic loading being a cumulative displacement of a section of the slope. Once the ground motion has ceased, no further deformation will occur unless the soil strength has been decreased significantly. As the induced deformations may be insignificant, the criterion that limiting equilibrium should never be exceeded would appear far too conservative. The choice of a static coefficient equivalent in effect to the dynamic loading, while an attractive concept, is impossible to evaluate. While it is possible that empirical values of the order of 0.1 could lead to safe slopes for a particular earthquake magnitude and certain types of soils, with little field experience to serve as a guide, and the lack of a method to assess their validity, their use would seem questionable.

With the development of dynamic response theories for earth embankments, various suggestions have come forth regarding their application in assisting with the selection of the magnitude of static seismic coefficients for embankment or earth dam design. The use of these theories for this purpose is discussed by Seed and Martin (1966).

Deformation or Dynamic Approach:

In view of the deficiencies of the pseudo-static approach outlined above, it would seem logical to attempt to assess earth slope stability during an earthquake in terms of permanent deformations resulting from the earthquake. The necessity for such a method, which would involve the consideration of the entire time history of lateral forces acting on a slope, is further demonstrated by the experimental evidence which has shown that the strength mobilized by soils under dynamic loading, is a function of both the magnitude and number of stress cycles. Failure to consider this latter factor, would be a serious deficiency of any design procedure.

The concept of assessing earthquake stability in terms of resulting permanent deformations was first proposed by Newmark. The design criterion required permanent displacements occurring over a sliding zone to be less than a prescribed tolerable value. Newmark (1965) presented an analysis based on this concept for the case where displacements could be assumed to occur over a well defined slip plane, and where the soil was assumed to behave as a rigid-plastic material having a well defined yield point.

For this case, by integration of those portions of the dynamic lateral accelerations acting on the sliding mass, which lie above the yield acceleration, permanent displacements on the sliding surface may be evaluated. This approach has been used successfully in analysing results of shaking table tests on banks of cohesionless soil (Goodman and Seed (1966)). For cohesive soils, however, where significant permanent deformations may occur at stress levels less than the strength, permanent deformations could occur over a large area within a cohesive soil slope during an earthquake. As a result, an analytical evaluation of cohesive slope deformations due to an earthquake has yet to be developed. The analytical approach is further complicated by pore pressure increases during dynamic loading, which affect the deformation and strength characteristics during the course of the earthquake.

To overcome these difficulties, Seed (1966) has suggested an approach, where soil samples are subjected in the laboratory to stresses similar to those occurring on soil elements in the field both before and during the earthquake. The method is based on the use of dynamic stress controlled triaxial tests similar to those previously described. The various steps in the method are as follows:

(1) Soil samples are initially consolidated using principal stresses equal to those at points on a potential failure circle. These initial stresses are calculated by making use of a conventional static stability analysis.
(2) Samples are then subjected to a range of pulsating stress amplitudes to determine conditions leading to either failure or a

selected permanent deformation. Seed considers that 13% axial strain could be indicative of undesirable distortions in cohesive embankments. A selected number of pulses are used, depending on the duration of the particular "design" earthquake. The critical conditions are expressed in terms of the allowable maximum shear stress τ_{ff} (static and dynamic) acting on the potential failure circle, for the various initial stress conditions. This may be greater or less than the static shear strength, depending on the nature of the soil, the number of cycles used, and the failure condition selected.

(3) In order to determine whether actual maximum shear stresses acting on the failure plane during the design earthquake will reach the allowable values or not, Seed makes use of a further static stability analysis incorporating an equivalent static seismic coefficient. It is suggested that dynamic response analyses be used to compute the time history of average dynamic seismic coefficients acting on the sliding mass, with the equivalent static seismic coefficient for use in the stability analysis being equal to say 2/3 of the maximum dynamic value (Seed and Martin (1966)).

(4) As a result of the stability analysis, a factor of safety analogous to that determined in a normal static stability analysis is determined. By analysing a large number of potential failure surfaces, the minimum factor of safety could be found.

The method thus attempts to take into account the dynamic response of the slope to a design earthquake of given duration, and the particular deformation or strength characteristics of the soil during dynamic loading. Ellis and Hartman (1967) have illustrated the use of this approach in the design of earth structures associated with the San Luis Canal in California. However, their analyses were limited to taking into account dynamic strength characteristics in stability analyses, seismic coefficients being empirically assigned rather than being assessed from dynamic response analyses.

As a practical design tool, it is felt that the method proposed by Seed has the disadvantage of requiring the performance of a large number of dynamic triaxial tests in order to assess critical conditions leading to failure or a prescribed permanent deformation for various initial conditions. This could be economically justified only for a major earth structure such as a large earth dam. Also, while for compacted earth slopes it is possible to prepare a large number of uniform samples, for natural cohesive earth slopes, the possibility of obtaining large numbers of uniform samples is often remote due to non-homogeneous in situ conditions. Also in order to calculate factors of safety, the allowable maximum shear stresses τ_{ff} determined from the dynamic test program are compared with shear stresses on the potential failure plane, as determined from a static stability analysis incorporating an average seismic coefficient. However, as the changes in superimposed principal stresses are thought primarily responsible for pore pressure increases and associated permanent deformations, it is felt the method of laboratory simulation proposed herein, is preferable.

In view of the above it is felt that a simplified method of analysis is desirable, which would be suitable for routine earthquake resistant design of cohesive earth slopes. Such a method should, however, retain the desirable features of including dynamic response effects as well as the deformation and strength characteristics of the soil under dynamic conditions.

Development of Proof Test Analysis

In order to limit the number of dynamic triaxial tests necessary for analysis, it is felt that use could be made of a "proof test" concept. Such a concept has been suggested by Taylor (1967) for earthquake resistant design of spread footing on cohesive soils. With this procedure, tests would simulate actual stresses resulting from the "design" earthquake at various points within the slope. The safety of the slope would then be assessed in terms of the sample behaviour observed. Obviously if samples fail, some concern must be felt regarding the safety of the slope during the earthquake. If samples do not fail, or deform a significant amount during the tests, then it is reasonable to assume that the slope is likely to be essentially stable. In view of the present inability to quantitatively correlate sample behaviour and field performance under earthquake loading and considering all the assumptions necessary to simulate earthquake stresses in the lab, it is felt unrealistic to attempt to put some quantitative figure on a factor of safety. Rather it is better to use one's engineering judgement having observed the results of laboratory tests, to decide whether the slope is satisfactory, or whether preventative measures or more conservative design is required.

The following outlines the proof test procedure:

Initial Sample Stresses: The first stage of the test procedure is to consolidate samples using stresses representative of in situ conditions. Consider a soil element on a potential failure surface, as shown in Fig. 12. The initial consolidation stresses σ_{1c} and σ_{3c} may be obtained either from either some form of elastic solution as previously described, or from a static stability analysis. Normally a long term static stability analysis would be in terms of effective stress and would be based on the method of slices. Hence one could determine the magnitude of the normal effective and shear stresses on the base of the slice, and by assuming the failure surface is at an angle of $45 + \frac{\phi'}{2}$ to the plane of the major principal stress σ_{1c}, the magnitudes of σ_{1c} and σ_{3c} can be computed. (ϕ' = the apparent angle of friction in terms of effective stress.)

Design Earthquake: In order to compute dynamic stresses to apply to the sample, it is necessary in the first instance to select a "design" earthquake. If it is assumed that the fundamental mode dominates the magnitude of dynamic stresses, then the design earthquake may be characterised by an acceleration response spectrum and a duration. The current N.Z. code uses the El Centro (1940) earthquake as a "standard" for intensity and duration. However, as it would seem that the El Centro records were affected by the nature of the soil deposits at the recording site (Shepherd and Travers (1970)), and as a design earth-

quake should characterise bedrock motions, it is felt that the continued use of El Centro should be discouraged. Also, the El Centro record was characteristic of a Richter Magnitude 7 earthquake, whereas a truly great earthquake could have a magnitude of 8 in the vicinity of the epicentre.

Jennings, Housner and Tsai (1968) have suggested the use of simulated earthquakes to overcome the lack of strong motion accelerograms, and have generated several artificial earthquake records typical of earthquakes of various durations and intensities. It is not intended to enter in to the controversial topic of the probability of occurrence of earthquakes of various magnitudes throughout New Zealand. However, it is suggested that as Wellington lies in a highly active earthquake belt, an M8 earthquake lasting say 60 seconds could be taken as the "design" earthquake in the area. In the case of Auckland, the closest probable epicentre of an M8 earthquake would conceivably lie in the general area of the Coromandel Peninsula, a distance of about 40 miles from the centre of the city. (Low intensity earthquakes occurred in this area in 1970). Hence the maximum acceleration of bedrock motion would be somewhat less than that in the vicinity of the epicentre. Curves presented by Seed, Idriss and Kiefer (1969) suggest maximum accelerations could be reduced by a factor of 0.4.

Fig. 13(a) shows the smoothed acceleration response spectra for an artificial M8 earthquake generated by Jennings et al and that for the same earthquake with accelerations reduced by a factor of 0.4 For the former curve (characterising a Wellington earthquake) a damping factor of 0.2 is used, which would be appropriate for cohesive soils undergoing cyclic deformations of a large amplitude. For the latter curve (characterising an Auckland earthquake) a lesser damping factor of 0.15 is used, as the lower dynamic strain amplitudes in the responding soils would be expected to have a reduced damping factor. It is suggested that the "design" earthquake for Auckland have a duration of 30 seconds.

For code purposes, it would seem desirable to further simplify the design spectra. This has been done as shown in Fig. 13(b) using the form adopted in NZSS 1900, Ch. 8, 1965, for Public Buildings. It can be seen that the suggested code spectra for cohesive soil response may be obtained by multiplying the existing structural code values by a factor of 4. In the case of the structural code, "the design lateral force is scaled down by considerations of damping, ductility and elastic design stresses" (SANZ : MP2:1965 Commentary on Chapter 8 of NZSS 1900) Such considerations are, to a large extent, inapplicable to soil structures, as 'limiting equilibrium' methods, rather than elastic methods, are employed in design.

Number of Loading Cycles in Dynamic Test: Assuming that the fundamental period dominates the dynamic response of the slope to earthquake, then for a given "design" earthquake duration, the number of loading cycles could be obtained by dividing the earthquake duration by the fundamental period. As the fundamental period of the slope itself may only be computed by means of a finite element analysis, it is suggested that for the purpose of a design procedure, sufficient accuracy is obtained if use is made of the one dimensional elastic shear deformation theory for horizontal soil deposits. (Idriss and Seed (1968).) For a thickness H of soil (assumed uniform) above bedrock, the one-dimensional theory gives the fundamental period as

$$T_1 = \frac{4H}{V_s} \text{ seconds} \qquad (1)$$

where V_s = shear wave velocity of the soil.

Hence the number of loading cycles would vary for different sections of the slope, that is, the number of cycles would be smaller where the depth to bedrock is greater. This is certainly true for points well removed from the slope, and is felt to be a reasonable approximation in the vicinity of the slope.

For practical use, equation (1) may be simplified in the following manner.

The shear wave velocity

$$V_s = [G.g/\gamma]^{\frac{1}{2}} \qquad (2)$$

where G = elastic shear modulus
γ = unit weight of soil

As previously noted, equivalent elastic moduli for soils during dynamic loading are strain amplitude dependent. However, it has been found that for typical Auckland saturated clays, for dynamic strain amplitudes of the order of those that might be expected in a strong earthquake, $G \doteq 100\ c_u$, where c_u is the undrained shear strength of the clay. Taking an average unit weight for clays of 100 lb/cu.ft., and substituting for G and γ in equation (2), gives $V_s \doteq (g.c_u)^{\frac{1}{2}}$. Substituting for V_s in equation (1) gives

$$T_1 = \frac{4H}{(g.c_u)^{\frac{1}{2}}} \qquad (3)$$

For non-uniform slope materials, c_u could be taken as the average undrained shear strength over the vertical section being considered.

Cyclic Stress Amplitudes: It was suggested in discussing the problem of laboratory simulation, that the magnitude of the cyclic deviator stresses be set equal to about 2/3 of the maximum earthquake value, this latter figure being approximated as twice the magnitude of the maximum horizontal shear stress at the point of interest. Although the maximum horizontal shear stress could be determined by a finite element analysis, it is suggested again, that for the purpose of routine design, use be made of an approximate estimate given by the theory for horizontal soil deposits. Taking the fundamental mode contribution, as approximating maximum response values, (the fundamental contributes about 85% for the problem shown in Fig. 5) then from the one-dimensional shear deformation theory, it can be shown that

$$\tau_{max.y} = \frac{8\gamma H\ k_{max}}{\pi^2} \sin \frac{\pi y}{2H} \qquad (4)$$

where y = depth of soil element below surface (see Fig. 12)

k_{max} = maximum seismic coefficient from design spectrum corresponding to the calculated period T_1 (equa. (3))

$\tau_{max.y}$ = maximum horizontal shear stress at depth y from the surface.

Taking γ = 100 lb/cu.ft., then from equation (4), the magnitude of the cyclic deviator stress to apply during a dynamic test is given by

$$\sigma_{d.dyn.} = 2/3 \times (\tau_{max.y}) \times 2$$

$$= 100\ k_{max}\ H \sin \frac{y}{2H} \qquad (5)$$

In order to check the degree of approximation given by the use of the one dimensional theory, a comparison was made with maximum horizontal shear stresses computed for the example shown in Fig. 4, using a finite element analysis, and those given by equation (4), where values of k_{max} were obtained from the acceleration response spectra for the El Centro earthquake (ordinates ÷ 2) with 20% damping. Natural periods were computed using equation (1), with H equal to the height of the slope surface above bedrock for the vertical section being considered. Results of the comparison are shown in Fig. 14. It may be seen that there is reasonable agreement considering the approximations that have been made, except that in the vicinity of the toe of the slope, shear stresses given by the one dimensional theory become zero whereas the finite element theory gives stresses of a reasonable magnitude. However, it should be noted that the accuracy of the finite element theory is in doubt at this point of stress concentration. Due account of possible errors in this region could be made if simulated tests of soil elements in the vicinity of the toe were being considered.

Permissible Permanent Deformations.

Naturally, if any sample fails during simulated earthquake loading, some concern must be felt for the safety of the slope during an earthquake similar to that assumed for design, and it is suggested that preventive measures such as increasing the static factor of safety of the slope be considered. However, it should be borne in mind that the failure of one sample does not necessarily mean the slope will fail, as this condition will depend on the complex interaction and stress redistribution which will necessarily occur if failure conditions are reached at one point in the slope while other points remain in a comparitively stable condition. At this stage, such effects cannot be considered in a quantitative manner. If samples do not fail, but deform significantly during simulated dynamic testing (say permanent axial strains > 15%), it is suggested that provided average permanent sample deformations obtained from tests at a series of points over a potential failure surface, do not exceed 10%, then the slope may be considered reasonably safe under earthquake conditions.

Example of Use of Proof Test Procedure

To illustrate the use of the proof test procedure, the results of tests carried out on two soil samples taken from a proposed motorway cutting in Auckland, are shown in Fig. 15. The potential failure surface shown was the critical circle computed using an effective stress analysis for long term static conditions. The static factor of safety with respect to the effective stress strength parameters equals 1.57. It should be noted that the critical failure surface under static conditions would not necessarily be associated with the maximum permanent deformations during simulated earthquake loading.

Samples: Undisturbed test samples were obtained using 4 inch thin walled sampling tubes, from a bore in the vicinity of point A. Samples for simulating conditions at points A and B were taken at or near the appropriate depths.

Test stresses: Initial consolidation stresses were obtained from the long term static stability analysis as previously described. The magnitude of the applied dynamic deviator stresses for each test were obtained using equation (5), the values of k_{max} for use in this equation being obtained using the Zone C design spectra shown in Fig. 13b. Values of the natural periods were obtained using equation (3), with H equal to H_A and H_B for the two test points as shown in Fig. 15, with c_u computed as the average value of undrained shear strength over each section considered. These strengths were those prior to construction of the cutting, but would be sufficiently accurate for the design procedure. The periods computed were used to obtain k_{max} values from the design spectra, and to calculate the number of cycles to apply in tests.

Test equipment: The apparatus, described in more detail in a previous publication, (Taylor, 1967)) is a stress-controlled dynamic triaxial compression machine in which a sinusoidally-varying dynamic axial load, combined with a constant (static) load can be applied to a sample (usually 3in. diameter by 6 in. long) in a triaxial cell. The dynamic loading is provided by a system of springs under-going sinusoidal deformation of adjustable frequency. The static load is applied by oil pressure acting on a piston (using a 'Bellofram' and hence having negligible friction).

Test procedure: Each sample was first allowed to consolidate under applied major and minor principal effective stresses estimated to be those acting, under static conditions, at the point within the slope under consideration. The deviator stress was provided by the loading piston. When consolidation was complete, further drainage was prevented. The required number of cycles of dynamic loading was then applied while load, deformation and pore-water pressure were determined using transducers, and recorded. The loading frequency has been found to have little effect on the results and it was found convenient to use a frequency of 1 Hertz. The pore-water pressure increased during dynamic loading, but, in the tests described this increase was small. Following the dynamic test, by slowly increasing the pressure in the loading piston, the axial load was increased to failure, under undrained conditions. This part of the test determined the undrained strength after dynamic loading.

Test results: As may be seen from Fig. 15, the dynamic tests resulted in negligible permanent deformation. Pore water pressure

build-up during the dynamic tests was also negligible, (0.3 p.s.i. in both samples A and B) and undrained strengths as obtained from the static tests following dynamic loading are likely to have been little affected by the dynamic loading. In view of the comparitively small dynamic stress amplitudes, this is perhaps not unexpected, for as can be seen from Fig. 8, the sum of the static and dynamic deviator stress needs to approach the undrained compressive strength to induce significant permanent deformation or failure for dynamic loadings involving between 10-100 cycles.

It should be noted that these test results comprised only a portion of the overall investigation. Deeper failure surfaces were also considered.

Conclusions

Failure of cohesive earth slopes during earthquakes, especially those associated with road and rail cuttings or embankments, may result in considerable inconvenience. For major works, it is suggested that the approach to aseismic design should take into account both the dynamic response characteristics of the slope and the dynamic strength characteristics of the soils involved. The proof test analysis outlined provides a convenient means of taking both of these factors into account.

In using the method, some judgement is necessary in deciding whether limiting equilibrium methods (i.e. static stability analyses) or elastic stress distribution solutions should be used to determine initial sample stresses. The finite element elastic solutions presented by Duncan and Dunlop (1969) have indicated that the stress conditions estimated from limiting equilibrium analyses can deviate considerably from those given by elastic theory, particularly in the case of cuts in over-consolidated clays.

Although the method necessitates dynamic triaxial tests, it is apparent that a preliminary appraisal of stresses involved may indicate the slope is safe without the need for dynamic tests. For example if the sum of the initial and dynamic deviator stresses are less than say 2/3 of the undrained compressive strength of the soil at a particular point in the slope under consideration, after consolidation at estimated in situ principal effective stresses, then as was indicated in the case of the design example described, permanent deformations induced by the dynamic loading are likely to be small.

It is apparent that low slopes resting on weak foundations soils with bedrock at a shallow depth, are particularly susceptible to earthquake damage. For such cases, natural periods are likely to be in the range of values giving maximum spectral accelerations, and the high dynamic shear stresses in the weak foundation soils could result in failure or considerable slumping of the slope.

Acknowledgements

The assistance of Tonkin and Taylor (Consulting Engineers, Auckland) in providing information and samples, and of the Ministry of Works in granting permission to publish the design example quoted, is acknowledged.

References

Ambraseys, N. N. and Sarma, S. K., "The Response of Earth Dams to Strong Earthquakes", Geotechnique, Vol. 17, No. 3, Sept. 1967, pp. 181-123.

Chopra, A. K., "Earthquake Response of Earth Dams", J. Soil Mech. and Found. Div., A.S.C.E., Vol. 93, No. SM2, March 1967.

Chopra, A. K., Dibaj, M., Clough, R. W., Penzein, J., Seed, H. B., "Earthquake Analysis of Earth Dams", Proc. 4th World Conf. on Earthquake Engineering, Chile, 1969.

Douglas, J. S., "Damage to State Highways - -1968 Inangahua Earthquake" Bull. N.Z. Soc. for Earthquake Engineering, Vol. 1, No. 2, Dec. 1968.

Duncan, J. M. and Dunlop. P., "Slopes in Stiff-Fissured Clays and Shales", J. Soil Mech. and Found. Div., A.S.C.E., Vol. 95, No. SM2, Mar. 1969, pp. 467-492.

Ellis, W. and Hartman, V. B., "Dynamic Soil Strength and Slope Stability", J. Soil Mech. and Found. Div., A.S.C.E., Vol. 93, No. SM4, July 1967, pp. 355-376.

Goodman, R. E., and Seed, H. B., "Earthquake-Induced Displacements in Sand Embankments", J. Soil Mech. and Found. Div., A.S. C.E., Vol. 92, No. SM2, Mar. 1966, pp. 125-146.

Idriss, I. M., "Finite Element Analysis for the Seismic Response of Earth Banks", J. Soil Mech. and Found. Div. A.S.C.E., Vol. 94, No. SM5, May 1968, pp. 617-636.

Idriss, I. M., and Seed, H. B., "Response of Earth Banks during Earthquakes", J. Soil Mech. and Found. Div., A.S.C.E., Vol. 93, No. SM3, May 1967, pp. 61-82.

Idriss, I. M., and Seed, H. B., "Seismic Response of Horizontal Soil Layers", J. Soil Mech. and Found. Div., A.S.C.E., Vol. 94, No. SM4, July 1968.

Idriss, I. M., Seed, H. B., and Dezfulian, H., "Influence of Geometry and Material Properties on the Seismic Response of Soil Deposits", Proc. 4th World Conf. on Earthquake Engineering, Chile, 1969.

Jennings, P. C., Housner, G. W., and Tsai, N. C., "Simulated Earthquake Motions", Earthquake Engineering Research Laboratory Report, California Institute of Technology, April 1968.

Martin, G. R., "The Dynamic Response of Cohesive Earth Dams to Earthquakes", Proc. 5th Aust.-N.Z. Conf. on Soil Mech. and Found. Eng., 1967, pp. 121-131.

Newmark, N. M., "Effects of Earthquakes on Dams and Embankments", Geotechnique, Vol. 15, No. 2, June 1965, pp. 139-160.

Parton, I. M., and Smith, R. W. Melville, "The Effect of Soil Properties on Earthquake Response", Paper presented at the N.Z. National Conf. on Earthquake Engineering, May 1971.

Seed, H. B., "Soil Strength During Earthquakes", Proc. 2nd World Conf. on Earthquake Eng., Tokyo, 1960, Vol. I, p. 183.

Seed, H. B., "A Method for Earthquake Resistant Design of Earth Dams", J. Soil Mech. and Found. Div., A.S.C.E., Vol. 92, No. SM1, Jan. 1966, pp. 13-41.

Seed, H. B., "Slope Stability during Earthquakes", J. Soil Mech. and Found. Div., A.S.C.E., Vol. 93, No. SM4, July, 1967, pp. 299-323.

Seed, H. B., "Soil Problems and Soil Behaviour", Earthquake Engineering, (Robert L. Weigel - Coordinating Editor), Prentice

Hall, 1970, Chapter 10.
Seed, H. B., and Chan, C. K. "Strength of Clays under Simulated Earthquake Loading Conditions", J. Soil Mech. and Found. Div., A.S.C.E., Vol. 92, No. SM2, March 1966, pp. 53-78.
Seed, H. B., and Idriss, I. M., "The Influence of Soil Conditions on Ground Motions During Earthquakes", J. Soil Mech. and Found. Div., A.S.C.E., Vol. 95, No. SM1, Jan. 1969, pp. 95-137.
Seed, H. B., Idriss, I. M., and Kiefer, F. W., "Characteristics of Rock Motions During Earthquakes", J. Soil Mech. and Found. Div., A.S.C.E., Vol. 95, No. SM5, Sept. 1969.
Seed, H. B., and Martin, G. R., "The Seismic Coefficient in Earth Dam Design", J. Soil Mech. and Found. Div., A.S.C.E., Vol. 92, No. SM3, 1966, pp. 25-58.
Shepherd, R., and Travers, J. H., "Surface Layer Modification of Seismic Shear Waves", N.Z. Eng., Vol. 25, No. 2, Feb. 1970, pp. 36-39.
Taylor, P. W., "Design of Spread Footings for Earthquake Loading", Proc. 5th Aust.-N.Z. Conf. on Soil Mech. and Found. Eng., 1967, p. 221.
Taylor, P. W., and Bacchus, D. R., "Dynamic Cyclic Strain Tests on a Clay", Proc. 7th Int. Conf. on Soil Mech. and Found. Eng., Mexico 1969, Vol. 1, p. 401.
Taylor, P. W., and Hughes, J.M.O., "Dynamic Properties of Foundation Subsoils as Determined from Laboratory Tests", Proc. 3rd World Conf. on Earthquake Eng., 1965, Vol. I, p.1-196.

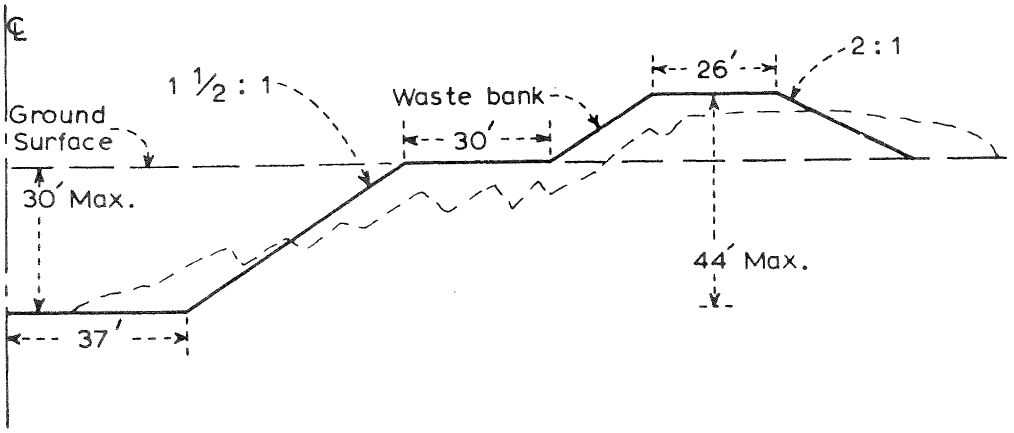

Fig. 1 BANK FAILURE -- ALL AMERICAN CANAL EL CENTRO EARTHQUAKE, 1940
(After Ellis and Hartman 1967)

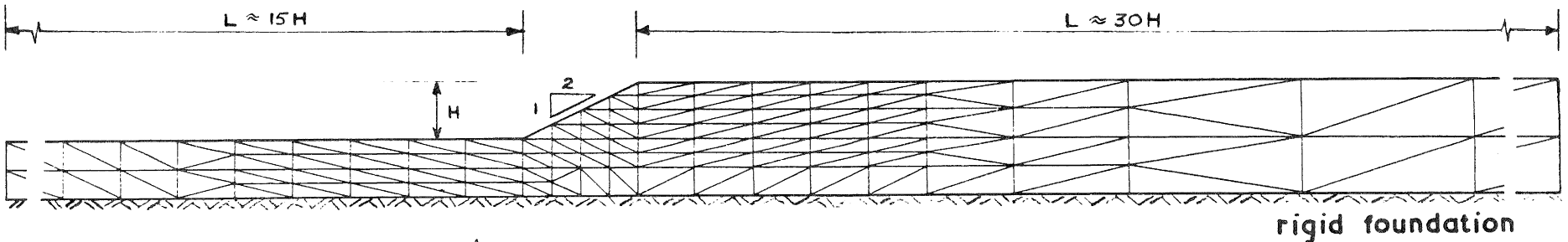

Fig. 2 FINITE ELEMENT IDEALIZATION OF EARTH BANK
(After Seed and Idriss 1967)

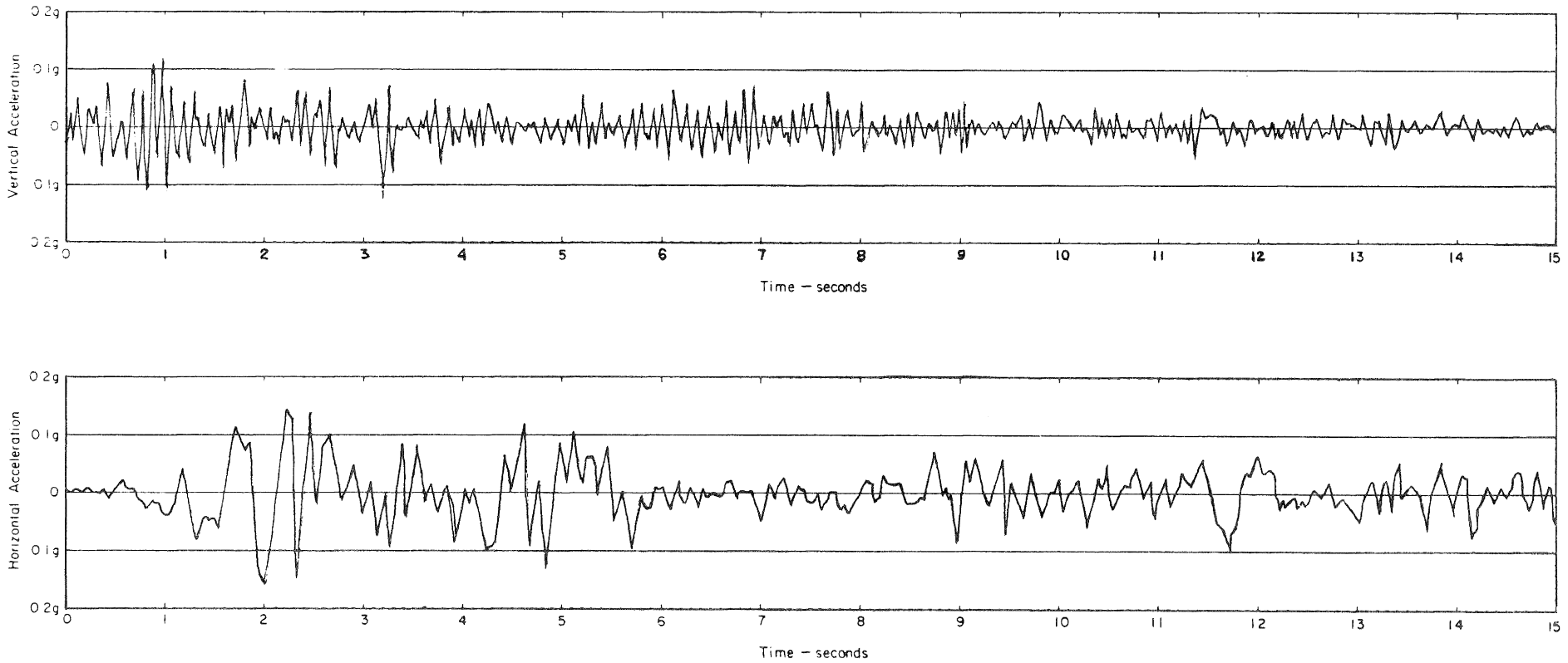

Fig. 3 EARTHQUAKE RECORD USED IN ANALYSES
El Centro N.S. 1940 – half intensity

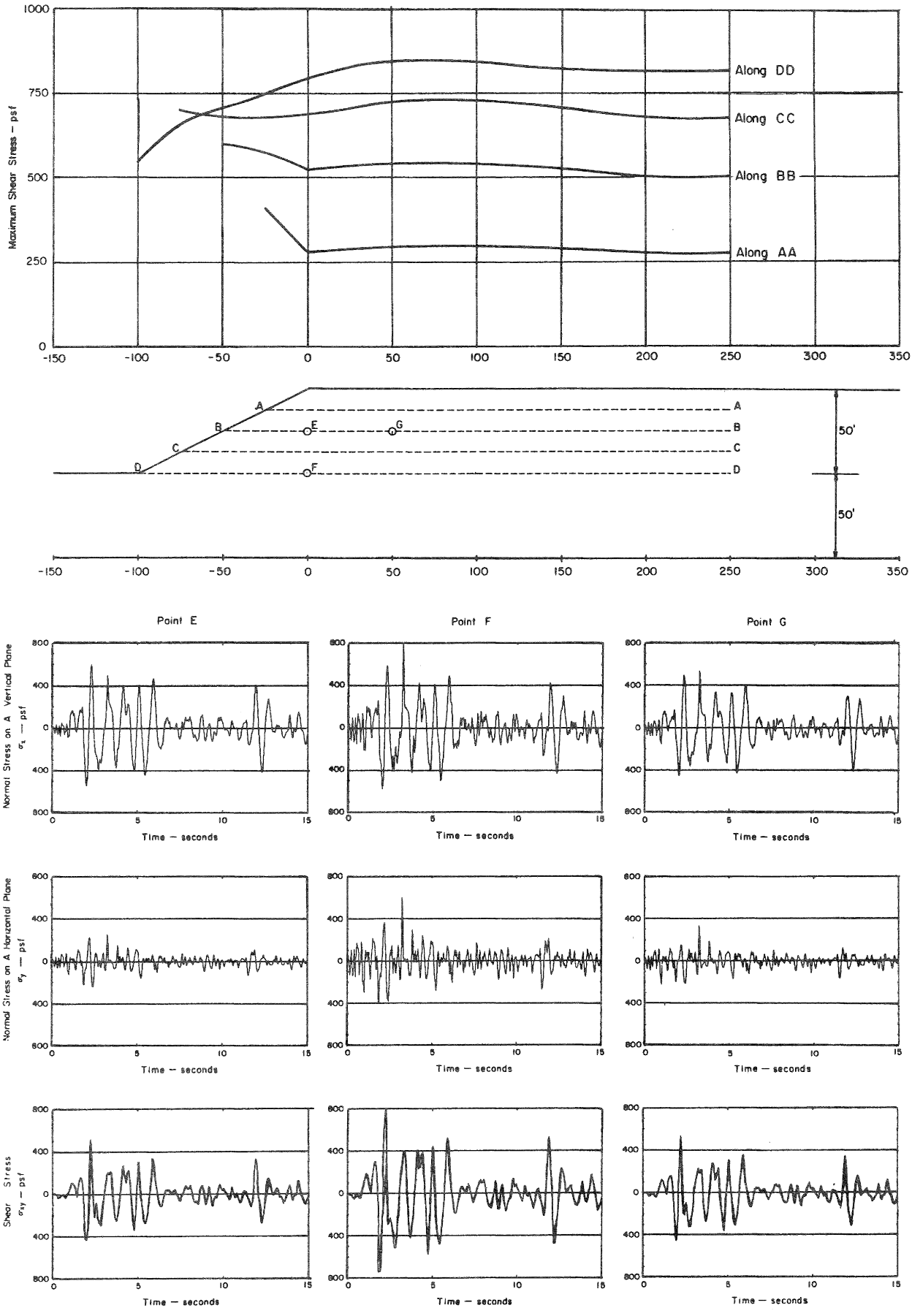

Fig. 4 STRESSES DEVELOPED IN EARTH BANK DURING EARTHQUAKE
(After Seed and Idriss 1967)

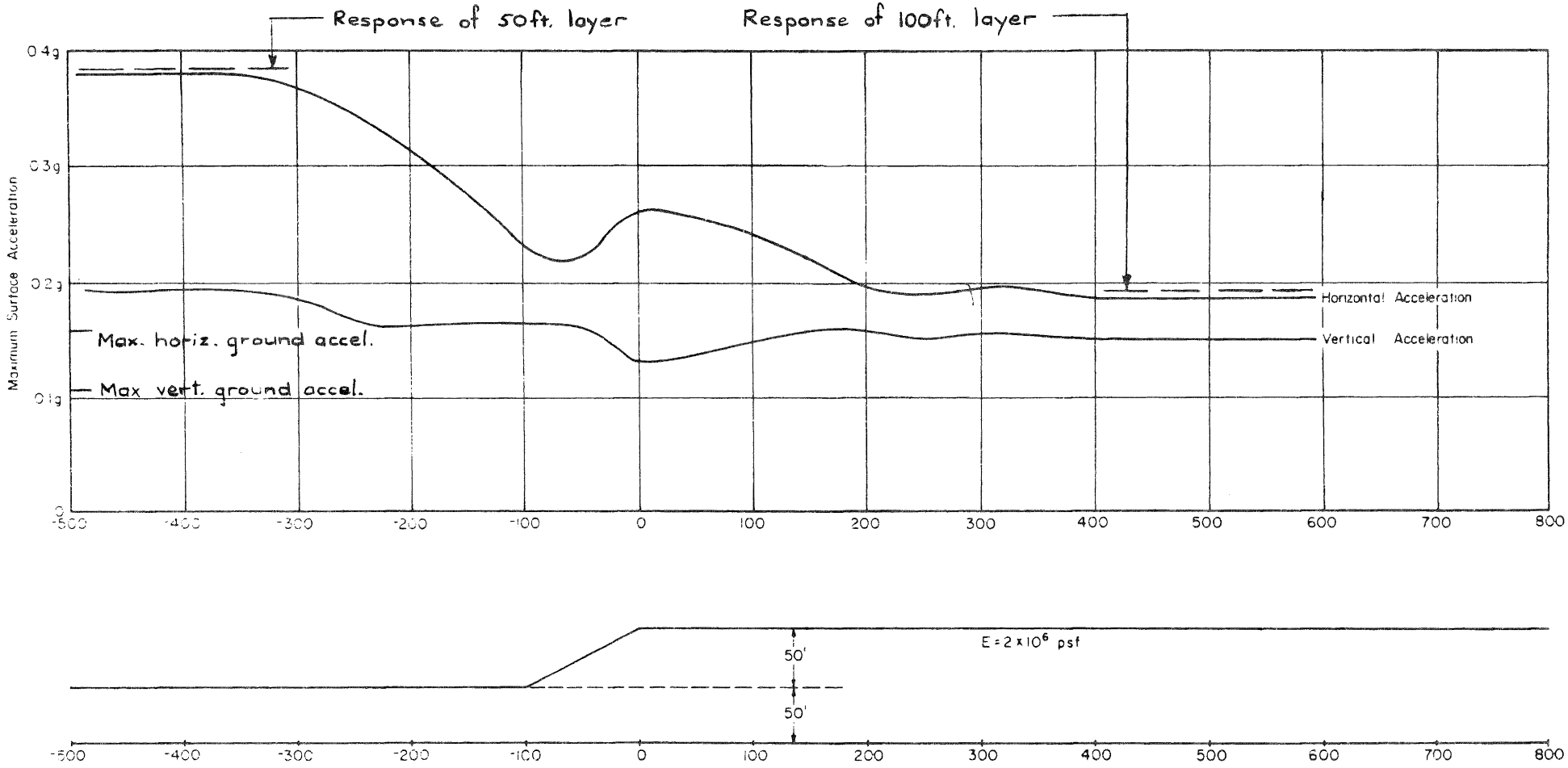

Fig. 5 MAXIMUM GROUND SURFACE ACCELERATIONS IN VICINITY OF EARTH BANK
(After Seed and Idriss 1967)

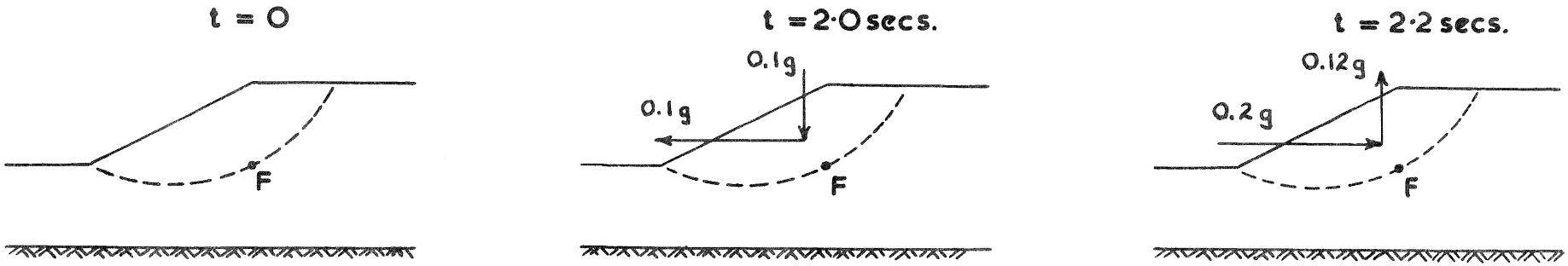

(a) Average lateral accelerations acting on sliding mass

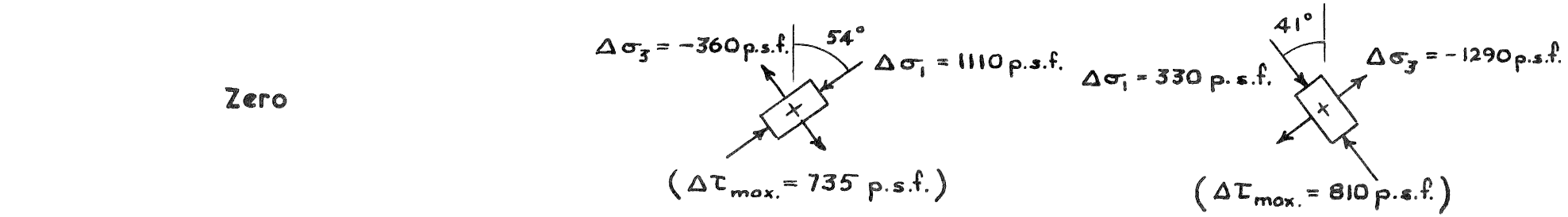

(b) Stresses induced by earthquake at point F

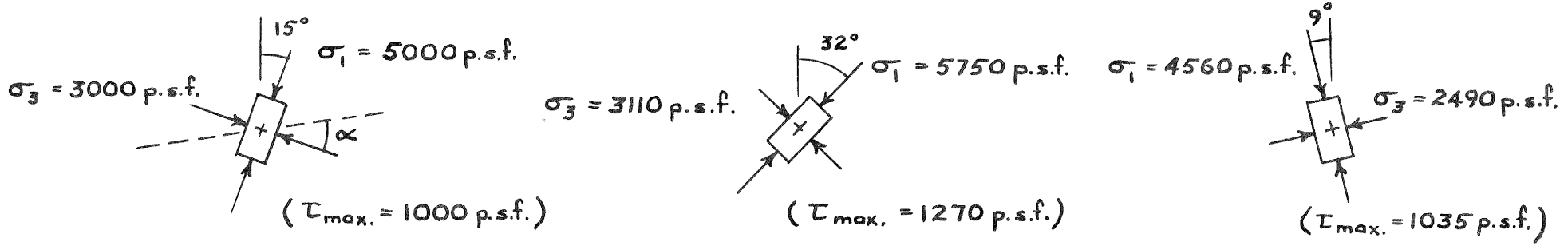

(c) Resultant stresses (static + earthquake) at point F

Fig. 6 PRINCIPAL STRESS REORIENTATION DURING EARTHQUAKE

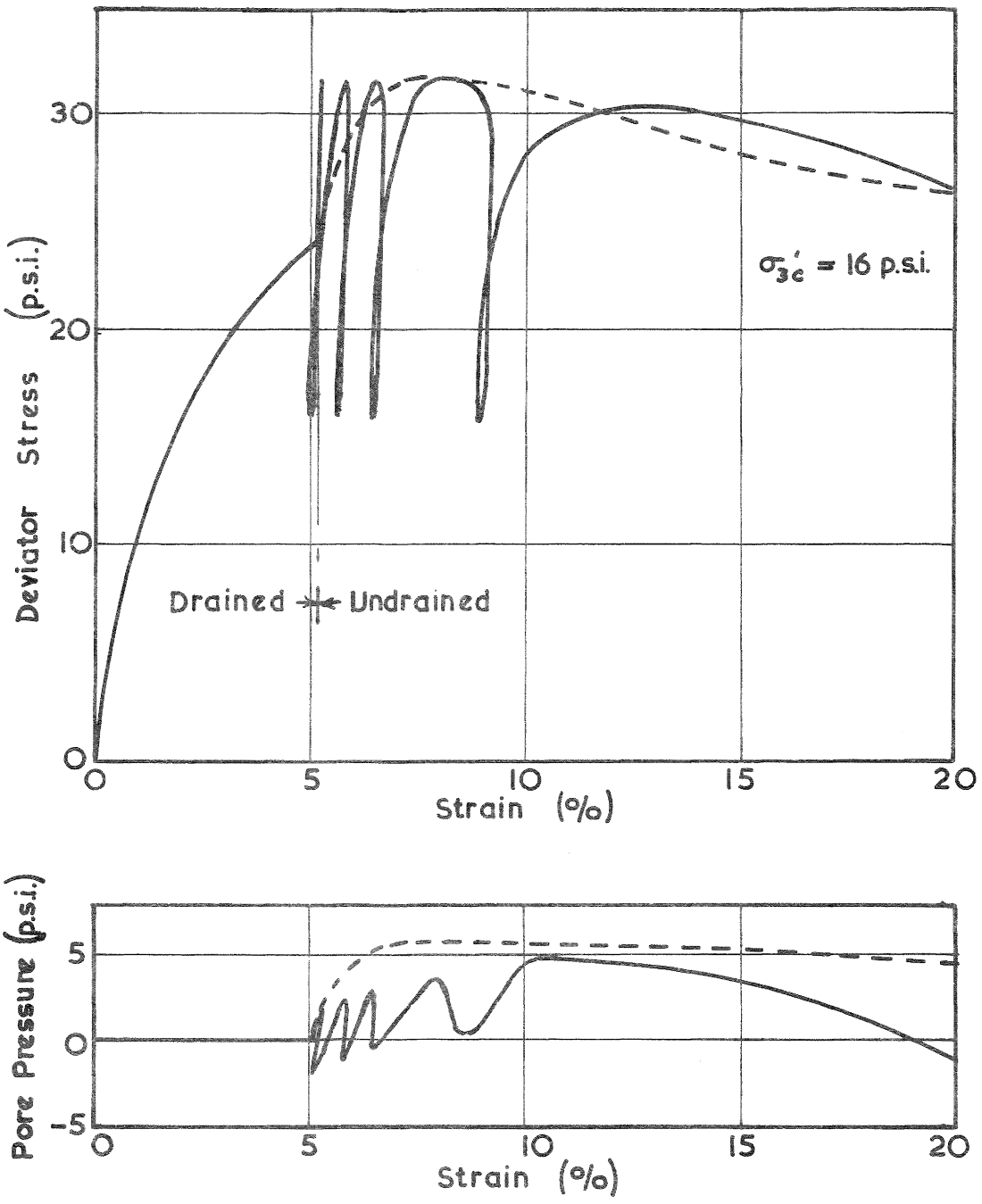

Fig. 7 STATIC AND DYNAMIC TRIAXIAL TESTS ON ANISOTROPICALLY-CONSOLIDATED SOIL

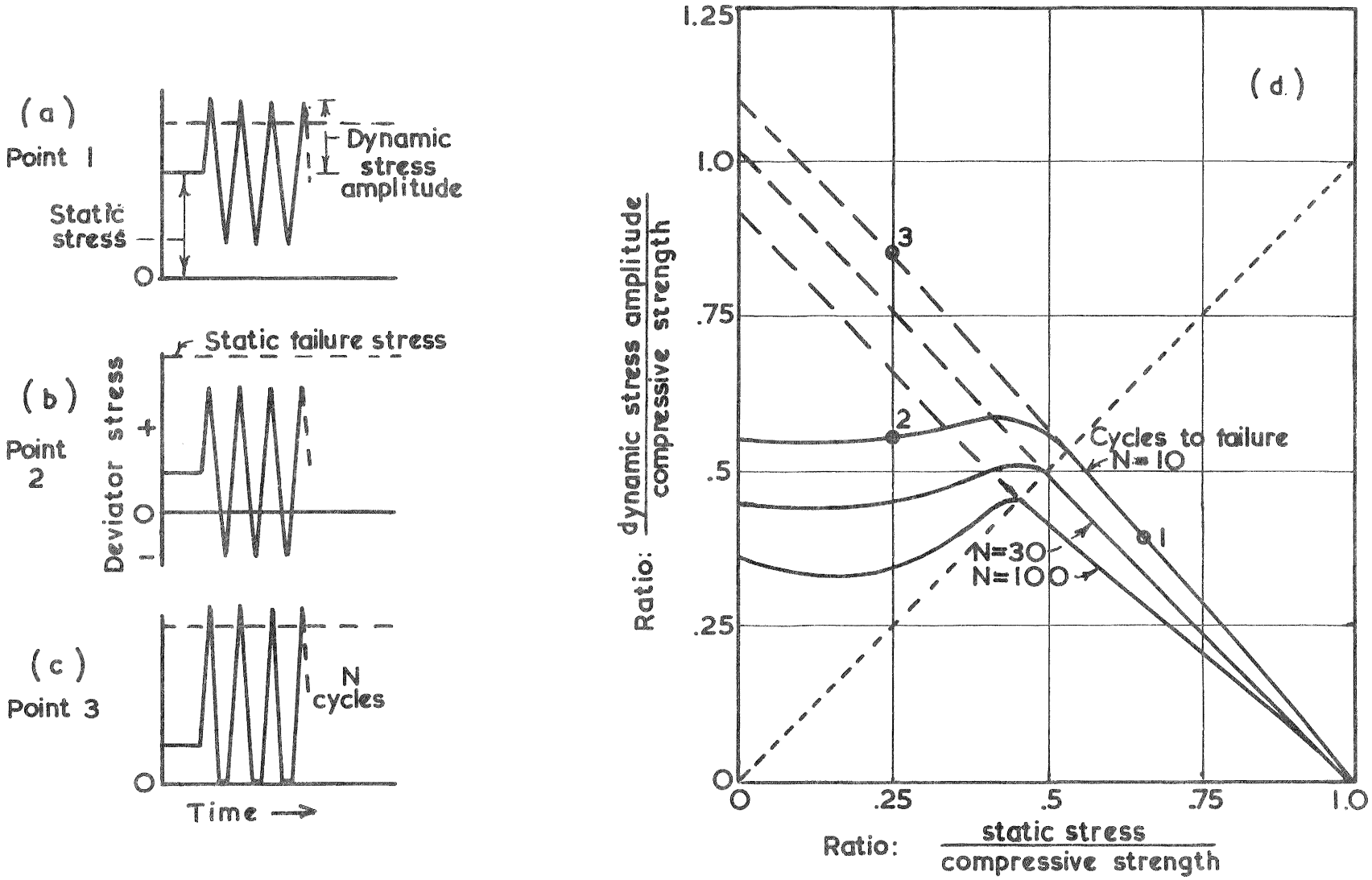

Fig. 8 DYNAMIC TRIAXIAL TESTS ON ISOTROPICALLY-CONSOLIDATED SOIL

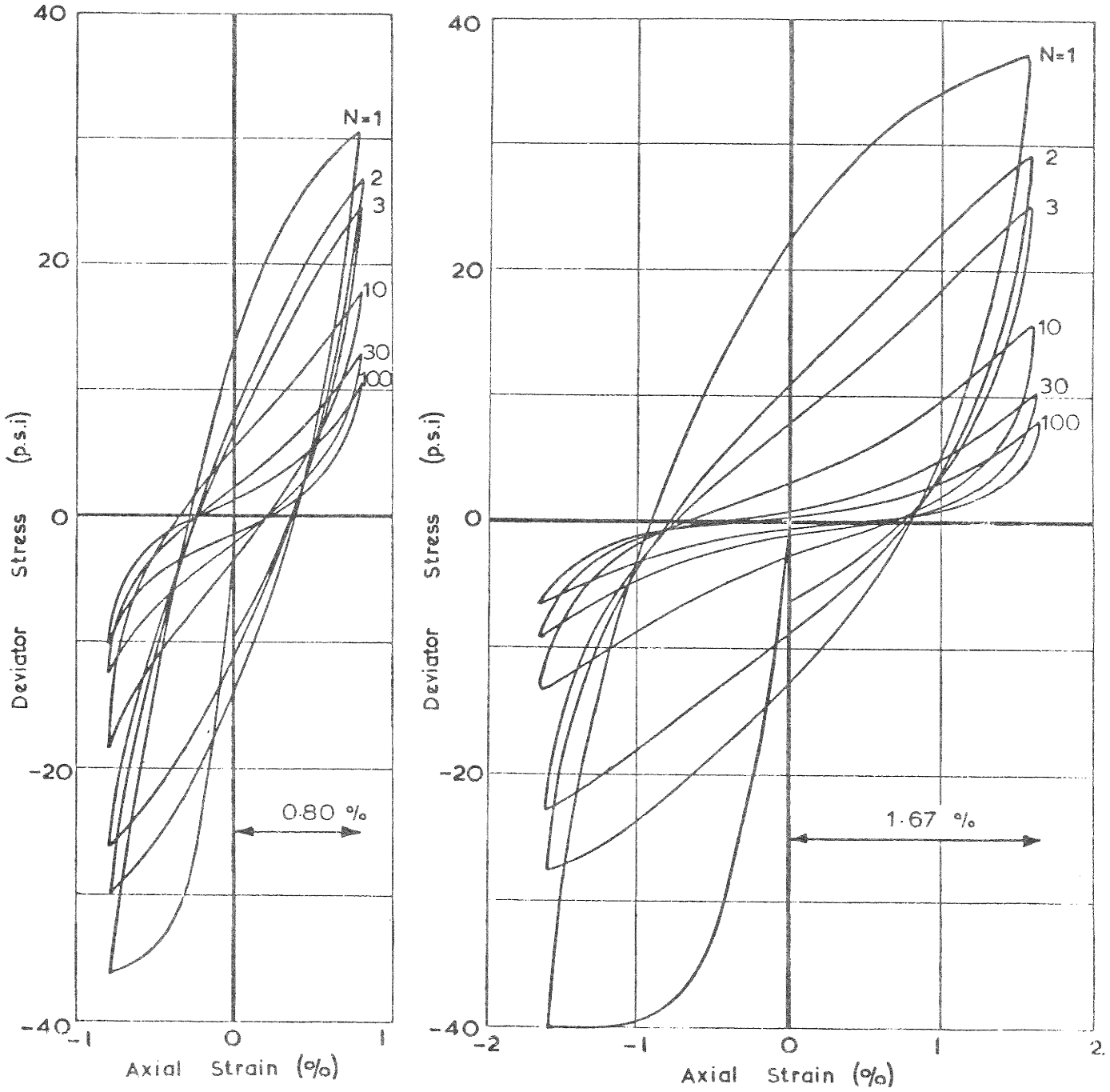

Fig. 9 TYPICAL LOAD DEFORMATION CHARACTERISTICS OF A SATURATED CLAY.

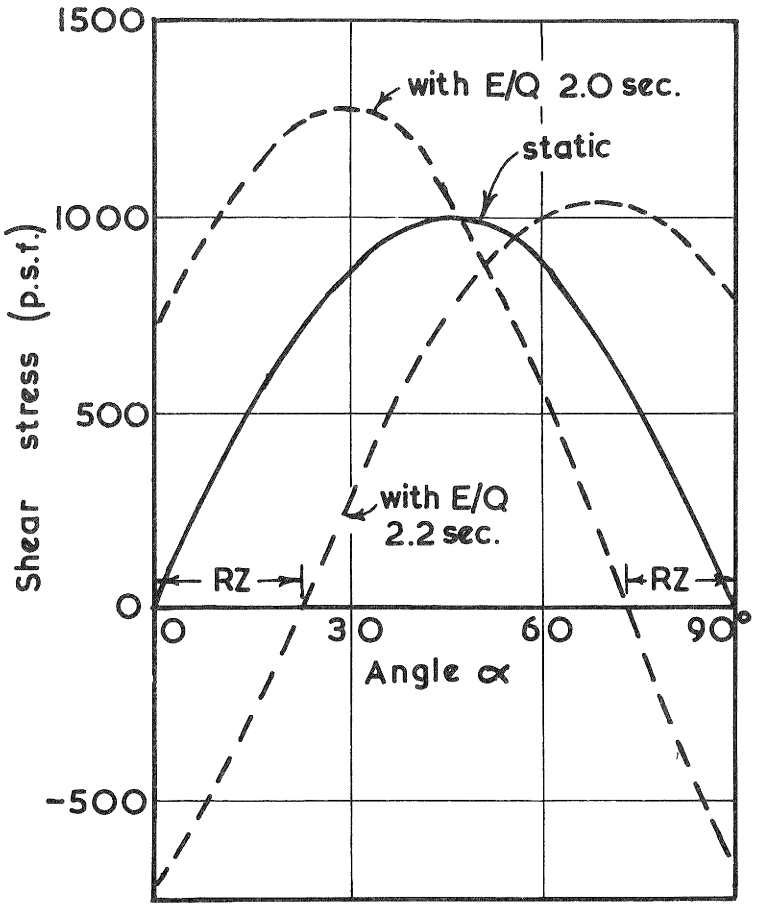

(a) Shear stress in the slope

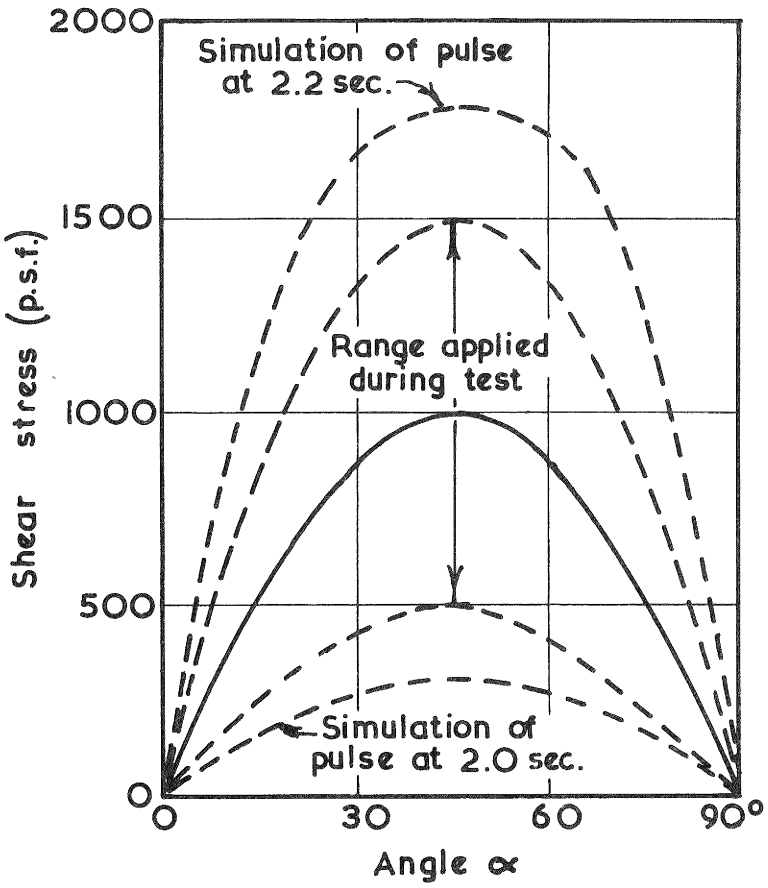

(b) Shear stress in the sample

Fig. 10 SHEAR STRESS vs. ORIENTATION OF PLANE

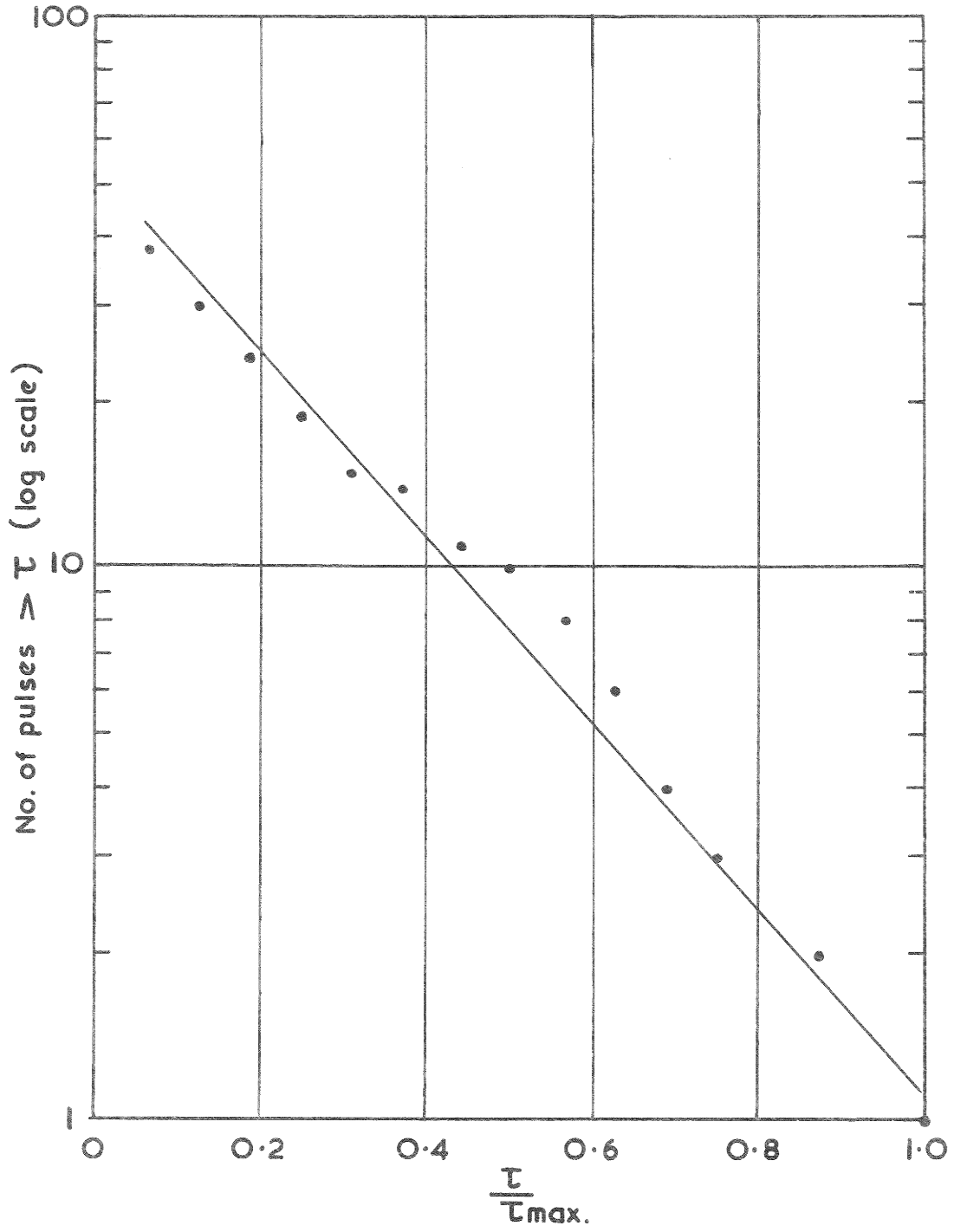

Fig. 11 DISTRIBUTION OF SHEAR STRESS PULSES

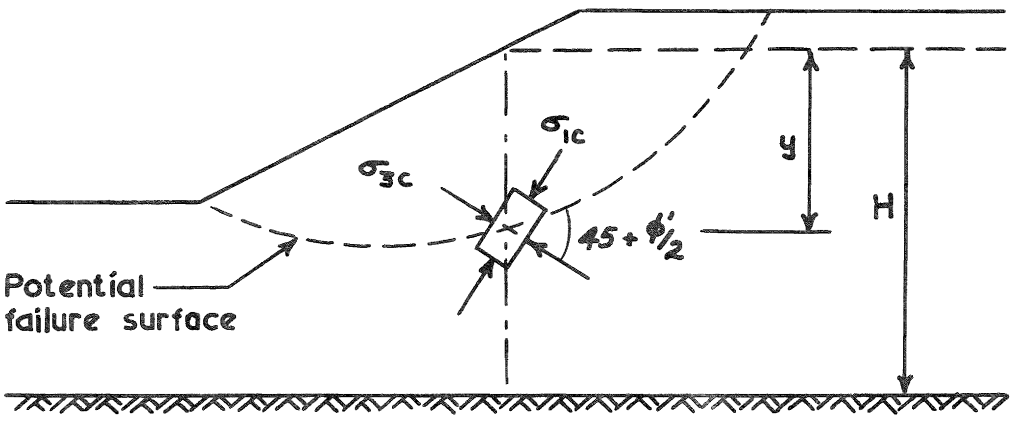

Fig. 12 PROOF TEST – INITIAL CONDITIONS

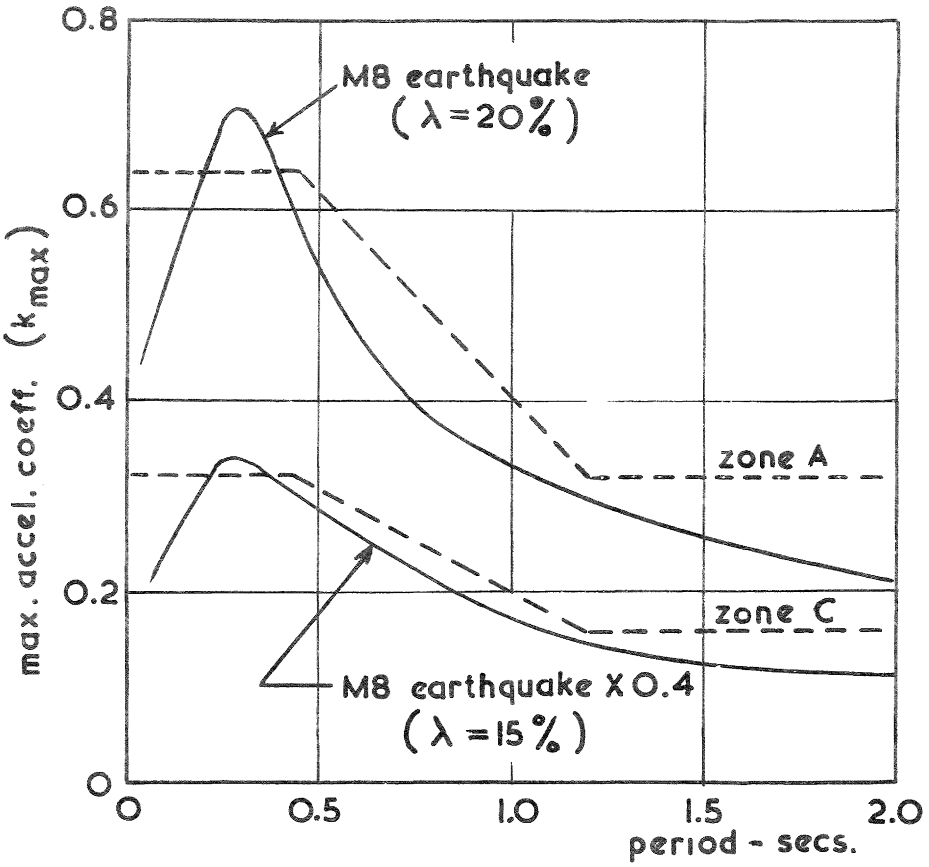

(a) Artificial earthquake spectra

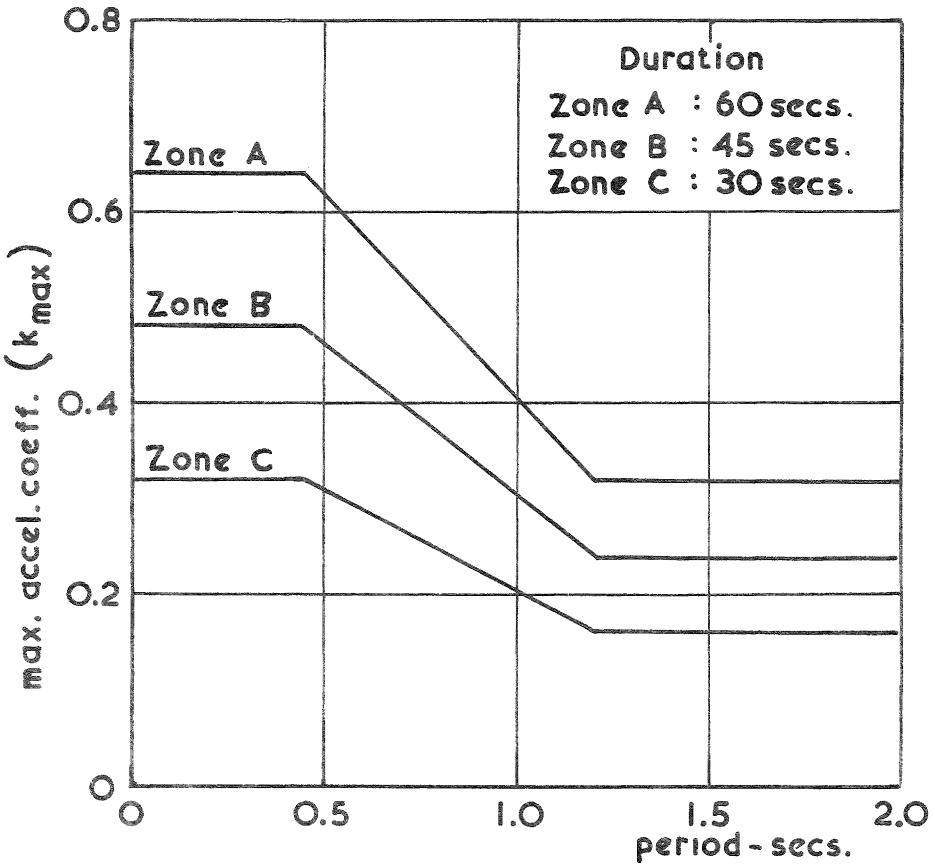

(b) Suggested code for cohesive soil response

Fig. 13 DESIGN EARTHQUAKE CHARACTERISTICS

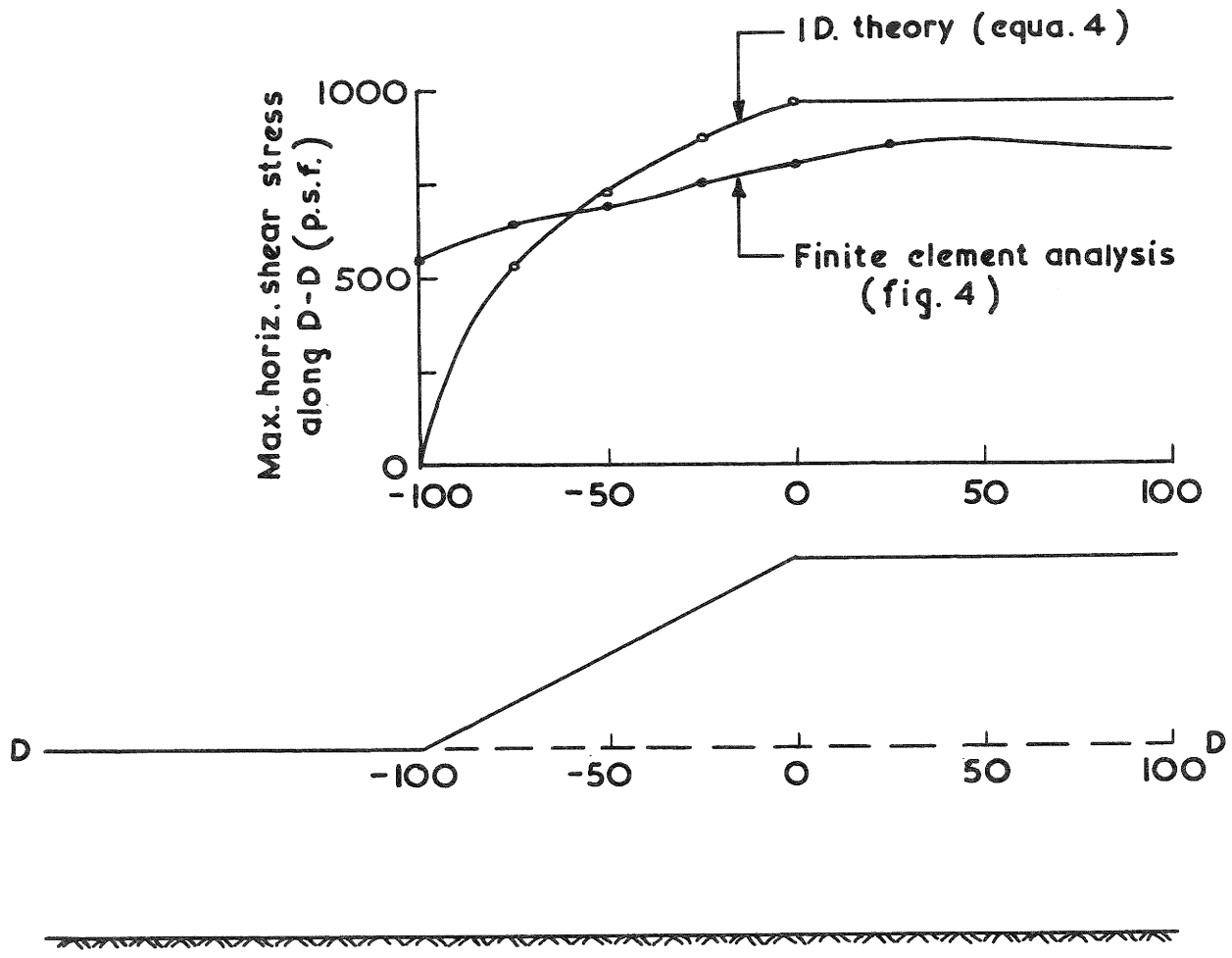

FIG. 14 COMPARISON OF HORIZONTAL SHEAR STRESSES

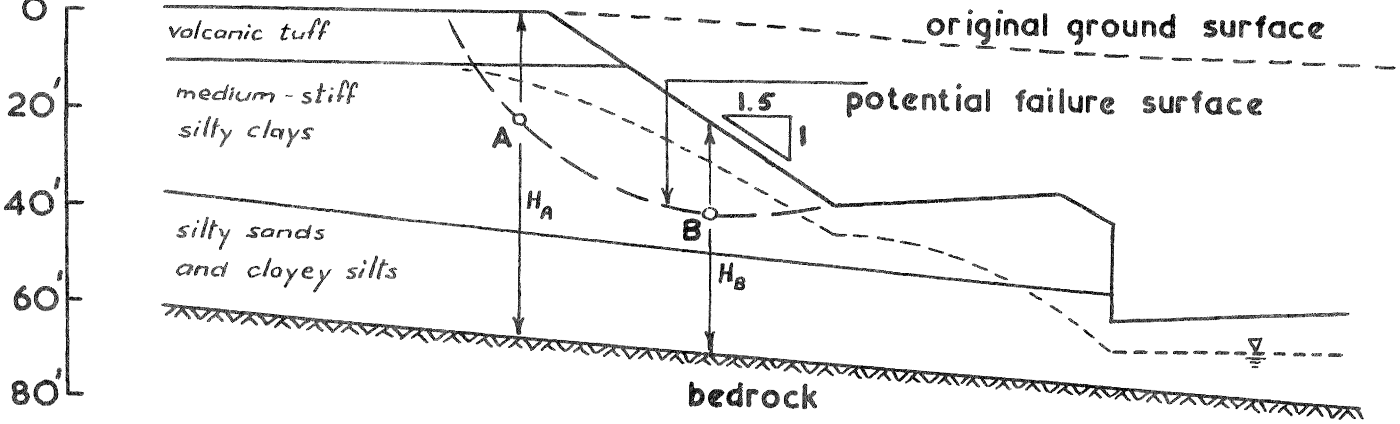

Section through motorway cutting

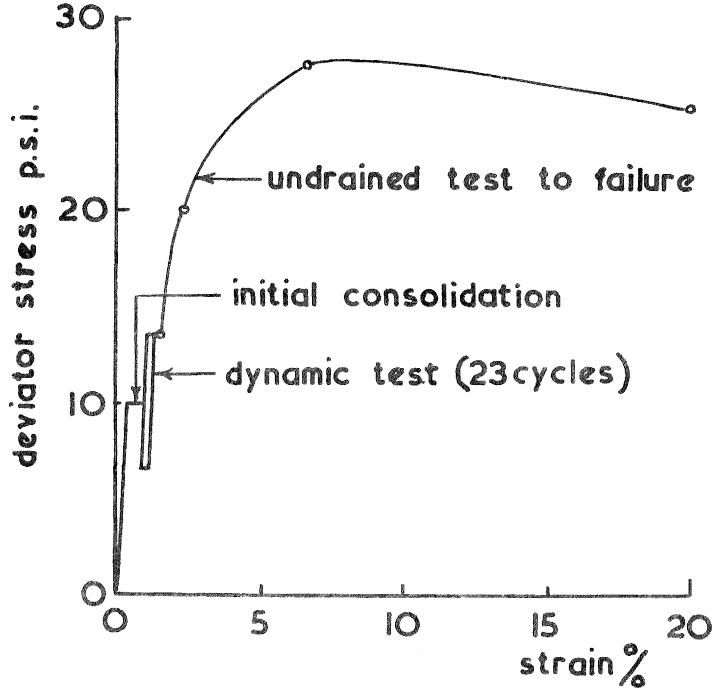

Test results — sample A

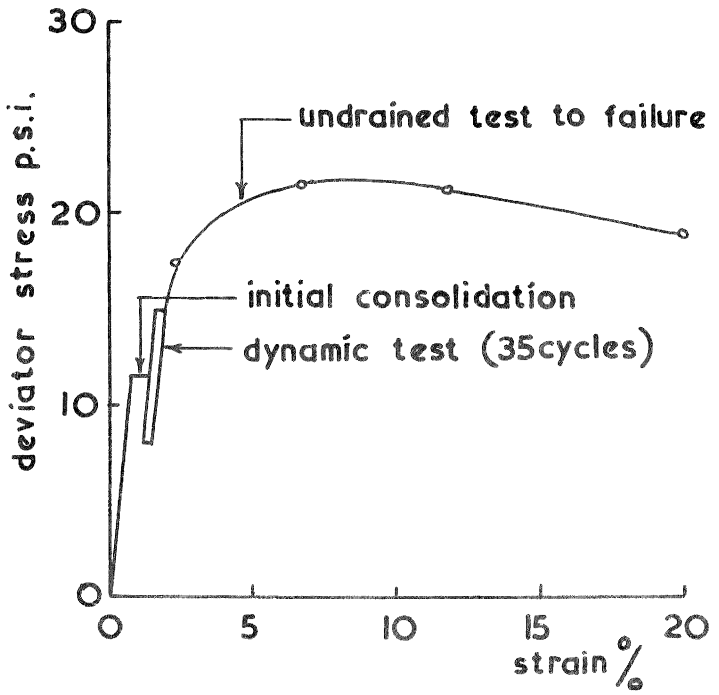

Test results — sample B

Fig. 15 PROOF TEST EXAMPLE